Cancer Biol Med 2025. doi: 10.20892/j.issn.2095-3941.2024.0385

ORIGINAL ARTICLE

Erianin inhibits the proliferation of lung cancer cells by suppressing mTOR activation and disrupting pyrimidine metabolism

Lili Yan[1]*, Yanfen Liu[1]*, Yufei Huang[1], Xiaoyu Sun[1,2], Haiyang Jiang[1], Jie Gu[1], Jing Xia[1], Xueni Sun[1,2], Xinbing Sui[1,2]

[1]School of Pharmacy and Department of Medical Oncology, The Affiliated Hospital of Hangzhou Normal University, Hangzhou Normal University, Hangzhou 311121, China; [2]Department of Gastrointestinal & Pancreatic Surgery, Key Laboratory of Gastroenterology of Zhejiang Province, Zhejiang Provincial People's Hospital, Affiliated People's Hospital, Hangzhou Medical College, Hangzhou 310014, China

ABSTRACT

Objective: Erianin has potential anticancer activities, especially against lung cancer. The specific mechanisms underlying the anticancer effects, including the molecular targets and signaling pathways in lung cancer, remain poorly understood and necessitate further investigation.

Methods: Lung cancer cell viability was evaluated using the CCK-8 assay. Flow cytometry was used to examine the effects of erianin on apoptosis and cell cycle progression. mRNA sequencing and metabolomics analysis were utilized to explore erianin-induced biological changes. Potential targets were identified and validated through molecular docking and Western blot analysis. The roles of mammalian target of rapamycin (mTOR) and carbamoyl-phosphate synthetase/aspartate transcarbamylase/dihydroorotase (CAD) in erianin-induced growth inhibition were studied using gene overexpression/knockdown techniques with uridine and aspartate supplementation confirming pyrimidine metabolism involvement. Additionally, lung cancer-bearing nude mouse models were established to evaluate the anti-lung cancer effects of erianin *in vivo*.

Results: Erianin significantly inhibits the proliferation of lung cancer cells, induces apoptosis, and causes G_2/M phase cell cycle arrest. Integrative analysis of mRNA sequencing and metabolomics data demonstrated that erianin disrupts pyrimidine metabolism in lung cancer cells. Notably, uridine supplementation mitigated the inhibitory effects of erianin, establishing a connection between pyrimidine metabolism and anticancer activity. Network pharmacology analyses identified mTOR as a key target of erianin. Erianin inhibited mTOR phosphorylation, thereby blocking downstream effectors (S6K and CAD), which are essential regulators of pyrimidine metabolism.

Conclusions: Erianin is a promising therapeutic candidate for lung cancer. Erianin likely inhibits lung cancer cell growth by disrupting pyrimidine metabolism by suppressing mTOR activation.

KEYWORDS Erianin; anti-cancer property; lung cancer; mTOR; pyrimidine metabolism

Introduction

Lung cancer is one of the most prevalent and lethal cancers worldwide[1-3]. Non-small cell lung cancer (NSCLC) represents approximately 85% of lung cancer cases, encompassing subtypes, such as adenocarcinoma and squamous cell carcinoma[4]. Treatment options for lung cancer include surgery, radiation therapy, chemotherapy, targeted therapy, and immunotherapy with surgical resection being the most effective treatment for early-stage cases[5-7]. Unfortunately, many lung cancer patients are diagnosed in advanced stages, which limits the effectiveness of conventional treatments. Platinum-based chemotherapy has been the standard for advanced lung cancer but is associated with severe toxic side effects and the risk of chemoresistance[8]. Because of these challenges, natural products have gained attention as potential therapeutic agents due to the multitargeted mechanisms and relatively low toxicity[9,10]. *Dendrobium chrysotoxum* Lindl. is a traditional Chinese medicine (TCM) and widely used in TCM practice. Erianin is

*These authors contributed equally to this work.
Correspondence to: Xueni Sun and Xinbing Sui
E-mail: xnsun@hznu.edu.cn and hzzju@hznu.edu.cn
ORCID ID: https://orcid.org/0000-0001-9958-2634 (X. Sun)
Received September 9, 2024; accepted January 3, 2025;
published online February 24, 2025.
Available at www.cancerbiomed.org

an active ingredient extracted from *Dendrobium chrysotoxum* Lindl. that has been shown to have anticancer activity in various types of cancer. Our previous studies highlighted the significant anti-cancer effects of erianin in lung cancer cells[11,12], which has prompted further investigation into the anti-lung cancer activity and underlying mechanisms.

One critical aspect of tumor cell proliferation is the biosynthesis of deoxyribonucleotides and ribonucleotides, which are essential for DNA and RNA synthesis. The *de novo* synthesis of pyrimidines is a key source of these nucleotides. Recent studies indicated that reprogramming of pyrimidine metabolism has a significant role in cancer progression and may represent a targetable vulnerability in cancer therapy[13,14]. The initial three steps of pyrimidine biosynthesis are catalyzed by CAD, a trifunctional enzyme with carbamoyl-phosphate synthetase, aspartate transcarbamylase, and dihydroorotase activities[15]. Dysregulation of CAD has been demonstrated in cancer and is related to poor clinical outcomes[16]. CAD activation occurs *via* mTOR through S6K-mediated phosphorylation at the S1859 site, promoting pyrimidine synthesis and cell cycle progression[17,18]. The mTOR pathway is a crucial signaling network that regulates cell growth, proliferation, and metabolism[19,20]. In cancer cells the mTOR pathway is often hyperactivated, resulting in uncontrolled growth, enhanced protein synthesis, angiogenesis, and therapeutic resistance[21]. Given the central role of the mTOR pathway in cancer biology, targeting the dysregulated mTOR pathway has emerged as a potential therapeutic strategy[22-25]. Drugs that inhibit mTOR signaling, such as temsirolimus[26] and everolimus[27,28], are currently under investigation in clinical practice and have shown promise in some cancer types.

In the current study transcriptome sequencing and metabolomics analyses provided compelling evidence that erianin exerts anticancer effects by modulating pyrimidine metabolism. Erianin targets mTOR and downregulates the mTOR-S6K-CAD signaling pathway, thereby modulating pyrimidine metabolism in lung cancer cells and subsequently suppressing growth. These findings highlight the potential of erianin as a therapeutic agent for lung cancer treatment and offer valuable insights into the molecular mechanisms of action.

Materials and methods

Materials

The cell lines used in this study [NCI-H460 (H460) and NCI-H1299 (H1299)] were obtained from the American Type Culture Collection [ATCC] (Manassas, VA, USA) and cultured in RPMI-1640 (Shanghai BasalMedia Technologies Co., Ltd, Shanghai, China) supplemented with 10% FBS (BIOVISTECH PTY. LTD., Sydney, Australia) in a 5% CO_2 cell culture incubator at 37°C. Erianin was obtained from Shanghaiyuanye Bio-Technology Co., Ltd. (Shanghai, China). Uridine and rapamycin were sourced from Shanghai Zeye Biotechnology Co., Ltd. (Shanghai, China). L-aspartic acid was obtained from Shanghai Canspec Scientific Instruments Co., Ltd. (Shanghai, China) and 3BDO (Shanghai, China).

Cell counting kit-8 (CCK-8) analysis

Cell viability was determined using a CCK-8 kit (Sigma-Aldrich, St. Louis, MO, USA). H460 and H1299 cells were seeded in 96-well plates at a density of 2×10^4 cells per well. After a 24-h incubation to allow for cell adhesion and growth, erianin was added to the wells at concentrations of 200, 100, 50, 25, 12.5, and 0 nM with the latter serving as the control representing no erianin treatment. Following a 24-h incubation, the culture medium (RPMI-1640) was replaced with fresh serum-free RPMI-1640 containing 10% CCK-8 solution. After an additional 4-h incubation with the CCK-8 solution, the absorbance of each well was measured at a wavelength of 450 nm using a microplate reader.

Apoptosis and cell cycle analysis by flow cytometry

The Annexin V-FITC (Yeasen Biotechnology (Shanghai) Co., Ltd., Shanghai, China) was utilized for apoptosis detection. Cell cycle experiments used the Cell cycle analysis kit [MULTISCIENCES (LIANKE) BIOTECH, CO., LTD., Hangzhou, China], which facilitated analysis of the cell cycle distribution. Following treatment, the cells were prepared and stained with the provided reagents from the kits per the manufacturer's instructions. Flow cytometry analysis was then performed on the stained cells using a flow cytometer.

Transcriptome sequencing and metabolomic analysis

RNA-seq analysis was carried out by Lianchuan Biological Information Technology Co., Ltd. (Hangzhou, China). RNA was extracted from both the erianin-treated and control groups after 24 h and transcriptome sequencing was

performed on the samples. Metabolomics analysis was performed by Wuhan Maiteville Biotechnology Co., Ltd. (Wuhan, China). The metabolome profiling utilized UPLC-Q-TOF-MS technology to analyze the differential metabolites between erianin-treated and untreated samples. Integrative analysis of the transcriptome sequencing and metabolomics results was performed using the MetaboAnalyst online tool (https://www.metaboanalyst.ca/).

Bioinformatic analysis

The putative targets of erianin were identified using the SwissTarget online tool (http://swisstargetprediction.ch/) based on the chemical structure of the compound, while potential therapeutic targets associated with lung cancer were sourced from the OMIM database. Pan-cancer analysis of mTOR expression was conducted using the Oncomine database. The UALCAN database was utilized to determine mTOR expression across different stages of cancer development. The Human Protein Atlas (HPA) database provided validation of the levels of mTOR protein expression in normal and lung cancer tissues. Molecular docking and dynamics simulations were performed to validate mTOR as a target of erianin. Crystal structures of mTOR were obtained from the Protein Data Bank (PDB) and utilized as initial configurations for the docking studies. The structure of erianin was obtained from PubChem. Protein and ligand preparation for molecular docking were conducted using the induced fit docking method.

Knockdown of CAD and overexpression of mTOR

CAD knockdown in lung cancer cells was accomplished through transient transfection with shRNA-CAD using Lipofectamine 2,000 (Invitrogen, Waltham, MA, USA), a widely used transfection reagent. The specific shRNA sequence utilized in this study was 5′-GCATATACGATACAAGGCTGTTAGAG-3′. Conversely, mTOR was overexpressed in lung cancer cells using an mTOR plasmid and Lipofectamine 2,000.

Western blot

Total protein was extracted from tissues or cells using a protein extraction buffer and the protein concentration was determined using a BCA protein assay kit (Beyotime, Shanghai, China) following the manufacturer's instructions. The proteins were subsequently separated by SDS-PAGE on a 10% polyacrylamide gel. The separated proteins were then transferred onto a PVDF membrane, which was subsequently incubated overnight with specific primary antibodies targeting the protein of interest. After washing to remove unbound antibodies, the membrane was incubated with a secondary antibody conjugated to an enzyme or fluorophore for 1.5 h. Protein bands on the PVDF membrane were visualized using an enhanced chemiluminescence reaget (New Cell & Molecular Biotech Co., Ltd., Suzhou, China) and captured with an exposure meter equipped with a chemiluminescence imaging system (BIO-RAD, California, USA).

Colony-formation assay

The cells were seeded at a density of 4,000 cells/6 cm dish and treated with erianin by replacing the culture medium with erianin-containing medium every 2 days for approximately 2 weeks. After colony formation the cells were fixed with 4% fixative solution and stained with 0.1% crystal violet solution. The colonies, visible as distinct violet-colored structures, were photographed using an appropriate camera.

Cellular thermal shift assay (CETSA)

H460 and H1299 cells were treated with DMSO or 100 nM erianin for 2 h. Following incubation, the samples underwent thermal cycling on a PCR instrument with a temperature gradient ranging from 55°C–80°C for 5 min. Thermal cycling was followed by five cycles of freeze-thawing in liquid nitrogen. After centrifugation, the supernatant was collected and mixed with SDS loading buffer, then heated at 100°C for 5 min in a metal bath. The prepared samples were stored at −80°C and subsequently analyzed by western blotting.

In vivo experiments

All animal experiments were performed in accordance with the guidelines of the Use and Care of Animals Committee at Hangzhou Normal University (HSD-20241203-01). Initially, 4×10^6 H460 cells were subcutaneously inoculated into mice to establish a lung cancer-bearing nude mice model. Erianin, dissolved in 50% dimethyl sulfoxide, was intraperitoneally injected into the mice at 50 mg/kg, 100 mg/kg, and 200 mg/kg doses during the pre-experiment phase. The mice in the erianin group were administered erianin at a concentration

of 100 mg/kg and uridine (33.4 g/kg) and 3BDO (0.05 g/kg) in corollary experiments. The tumor size was regularly monitored every 2nd day to track changes in tumor growth. The mice were sacrificed after 18 days of treatment and the tumors were harvested for further analysis.

Statistical analysis

The data were prepared and analyzed using GraphPad Prism (10.1.2). Cell line-based experiments were performed with three biological replicates per condition and the animal experiments included five replicates per group. Following assessment of normality, differences between the two groups with normal distribution were assessed using Student's t-test. For comparisons involving more than two groups with a normal distribution, an initial ANOVA analysis was performed followed by *post-hoc* pairwise comparisons using Tukey's multiple comparisons test. Statistical significance was set at a $P < 0.05$.

Results

Erianin inhibited lung cancer cell growth, induced cell apoptosis, and arrested the cell cycle in the G_2/M phase

Erianin has been shown to exert significant anticancer effects on lung cancer cells by reducing cell viability, inducing cell cycle arrest, and promoting apoptosis. In the current study the anticancer effects of erianin were validated using two lung cancer cell lines (H460 and H1299). The CCK-8 kit and flow cytometry were used to assess cell viability, cell cycle distribution, and apoptosis. To evaluate the effects of erianin on lung cancer cell viability, varying concentrations of erianin were administrated to H460 and H1299 cells and cell viability was measured using the CCK-8 assay after 24 h. Erianin significantly reduced the survival rate of both cell lines with IC_{50} values calculated at 61.33 nM for H460 cells (**Figure 1A**) and 21.89 nM for H1299 cells (**Figure 1B**). Furthermore, apoptosis analysis revealed that erianin induced apoptosis in lung cancer cells in a dose-dependent manner in both cell lines (**Figure 1C-E**), indicating the ability of erianin to trigger programmed cell death. As we reported in a previous study[12], erianin has also been shown to induce ferroptosis in lung cancer cells, indicating that apoptosis is not the sole mechanism contributing to erianin-induced cell death. Natural compounds like erianin often exert antitumor effects through multiple, potentially interconnected mechanisms, which may be influenced by factors, such as the compound mode of action, tumor cell type, and the surrounding microenvironment. Additionally, erianin significantly induced G_2/M phase cell cycle arrest in H460 and H1299 cells (**Figure 1F-H**). These findings collectively underscore the potent anticancer effects of erianin on lung cancer cells, highlighting the potential of erianin as a promising therapeutic candidate for lung cancer.

Erianin potentially affects nucleotide metabolism in lung cancer cells through targeting mTOR

Our previous study[12] in combination with the analyses presented herein have confirmed that erianin significantly reduces the viability of lung cancer cells, induces cell cycle arrest, and triggers apoptosis. However, the precise mechanisms underlying the anti-tumor effects of erianin are not completely understood. To address this knowledge gap and elucidate the potential mechanisms of action underlying erianin in lung cancer, H460 cells were treated with 100 nM erianin for 24 h, followed by transcriptomic sequencing and metabolomics analyses. As depicted in **Figure 2A**, **B**, these analyses revealed 12,627 differentially expressed genes and 59 metabolites in H460 cells when comparing the erianin-treated group to the untreated group. Further integrated analysis of these differentially expressed genes and metabolites using the MetaboAnalyst 6.0 online tool indicated that erianin significantly impacts nucleotide metabolic pathways in lung cancer cells, especially those pathways involved in purine and pyrimidine metabolism (**Figure 2C**). Nucleotides are critical for DNA and RNA synthesis and are essential for tumor cell growth and proliferation. These findings suggest that erianin may interfere with critical biochemical pathways involved in nucleotide synthesis and utilization, thereby inhibiting the growth and proliferation of lung cancer cells.

To further elucidate the pathway by which erianin affects nucleotide metabolism of lung cancer cells, an analysis of potential erianin targets in lung cancer was performed using network pharmacology. The SwissTarget online tool predicted 100 potential targets for erianin, while 200 potential therapeutic targets for lung cancer were identified through the OMIM database. These targets were subsequently analyzed using Venn cross-analysis, revealing three potential targets for erianin in lung cancer (EPHB2, mTOR, and KDM1A; **Figure 2D**). To further validate these targets, molecular docking and

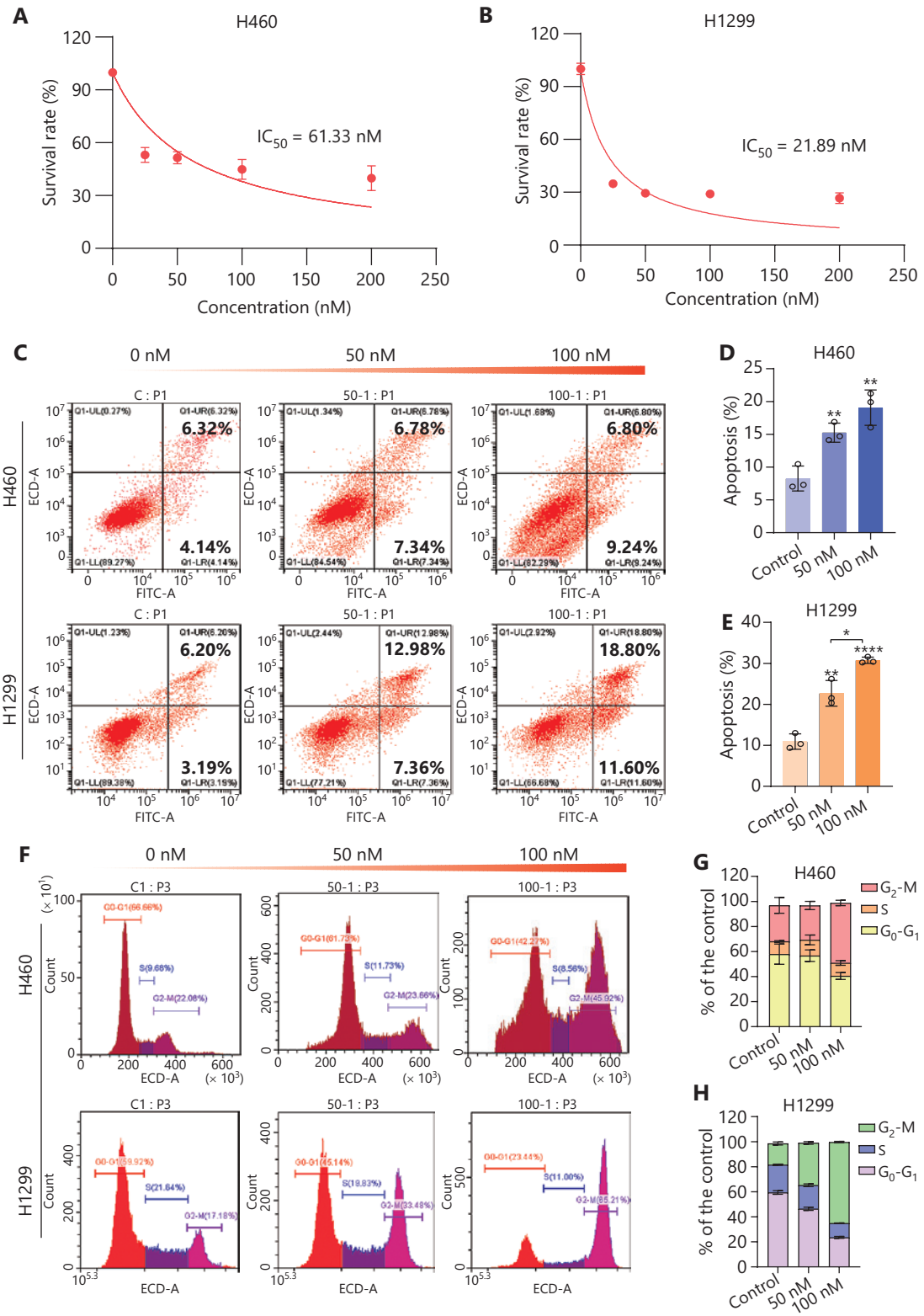

Figure 1 Illustration of the effects of erianin on lung cancer cell viability, apoptosis, and cell cycle distribution. (A) The IC_{50} value of erianin against H460 cells was determined using the CCK-8 assay. (B) The IC_{50} value of erianin against H1299 cells was determined using the CCK-8 assay. (C) Representative flow cytometric apoptosis staining after treatment with different doses of erianin (0 nM, 50 nM, and 100 nM) in H1299 and H460 cells is shown. (D-E) Quantitative analysis of cell apoptosis after treatment with different doses of erianin (0 nM, 50 nM, and 100 nM)

in H1299 and H460 cells is shown; mean ± SD, $n = 3$, *$P < 0.05$, **$P < 0.01$, ****$P < 0.0001$. (F) Representative flow cytometric analysis of cell cycle distribution after treatment with different doses of erianin (0 nM, 50 nM, and 100 nM) in H1299 and H460 cells is shown. (G-H) Quantitative presentation of cell cycle distribution after treatment with different doses of erianin (0 nM, 50 nM, and 100 nM) in H1299 and H460 cells is depicted. The data are presented as the mean ± SD, $n = 3$.

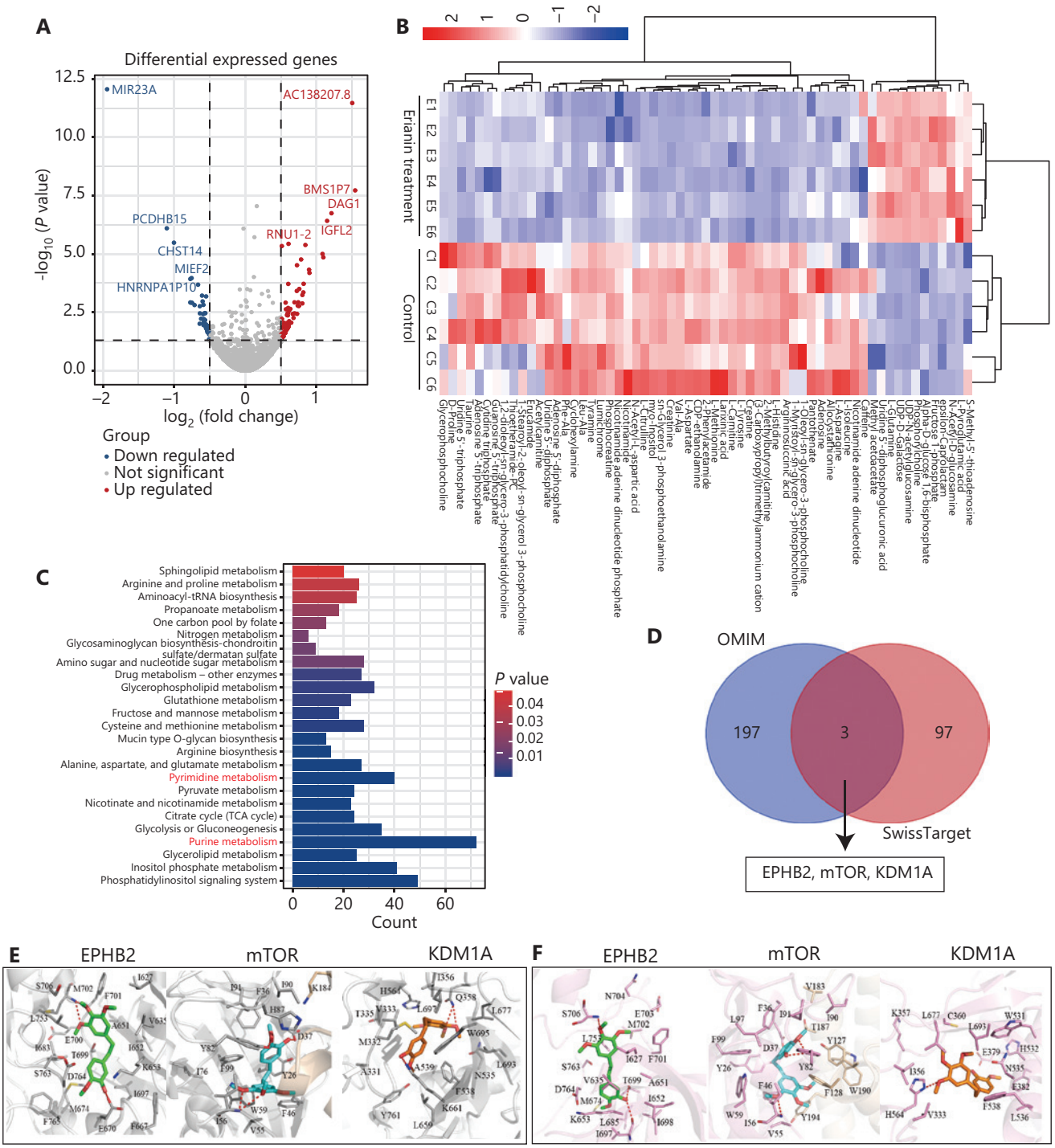

Figure 2 Continued

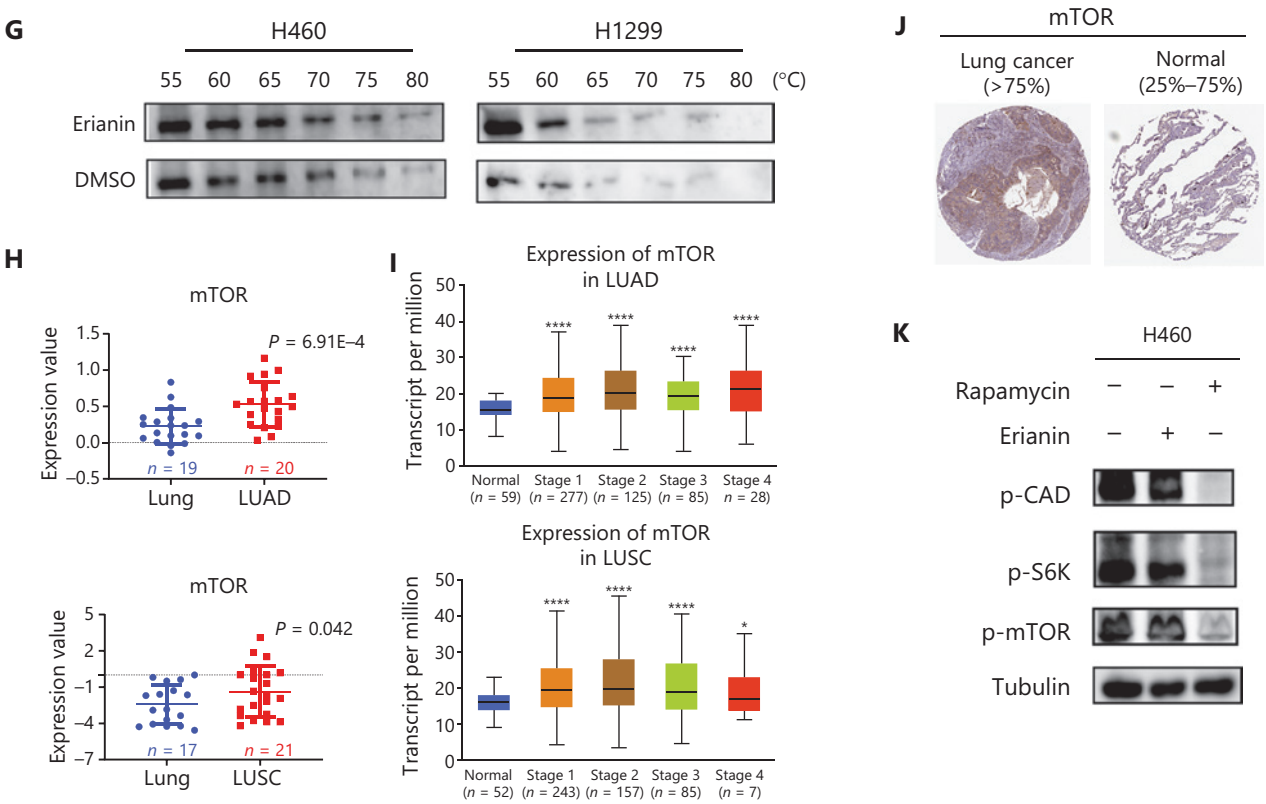

Figure 2 Erianin influences pyrimidine metabolism in lung cancer cells. (A) The volcano plot displays differentially expressed genes between control and erianin-treated H460 cells. Genes that are upregulated ($log_2FC > 0.5$) in erianin treatment groups are highlighted in red and genes that are downregulated ($log_2FC < -0.5$) are shown in blue. Genes with no significant change in expression are depicted in gray ($-0.5 < log_2FC < 0.5$). (B) The heatmap represents the differential metabolites between erianin-treated and -untreated H460 cells. Metabolites that are upregulated in erianin treatment groups are indicated in red and metabolites that are downregulated are indicated in blue. (C) The combined analysis of transcriptome and metabolome data using the MetaboAnalyst 6.0 online tool and visualized using the Hiplot online tool demonstrated that erianin impacts nucleotide metabolism in H460 cells. (D) Prediction of erianin targets in lung cancer. The OMIM database was utilized to predict the therapeutic targets of lung cancer and the SwissTarget online tool was used to predict the potential targets of erianin. The Venn diagram shows three potential targets of erianin in lung cancer. (E) Molecular docking study of the binding affinity of erianin to EPHB2, mTOR, and KDM1A. (F) Molecular dynamics simulations of the conformational changes. Red dashed lines indicate inferred hydrogen bonds. (G) The impact of erianin on the thermal stability of mTOR across various temperature gradients was assessed using CETSA in H460 and H1299 cell lines. (H) Analysis from the Oncomine database demonstrated upregulation of mTOR in lung cancers. Statistical charts were generated using GraphPad Prism 8 software. (I) mTOR expression was significantly upregulated across different cancer stages, $^*P < 0.05$, $^{****}P < 0.0001$. Data were obtained from the UALCAN database. (J) The level of mTOR protein expression was determined *via* immunohistochemistry staining from the HPA database and revealed increased expression of mTOR in lung cancer tissues compared to normal lung tissues. (K) Western blot analysis was performed to assess p-mTOR, p-S6K, and p-CAD after treatment with erianin (100 nM) or rapamycin [20 nM (positive control)] for 24 h.

kinetic simulations were performed to assess the interactions between erianin and EPHB2, mTOR, and KDM1A. Initial protein configurations (EPHB2 PDB ID: 3ZFM; KDM1A PDB ID: 5LHI; and mTOR PDB ID: 3FAP) were obtained from the PDB and the erianin structure was sourced from PubChem. The induced fit docking (IFD) method was used to account for receptor flexibility, which improved binding interaction predictions. The optimal binding conformations, which were based on affinity and energy evaluations, were selected to represent binding efficacy. Due to structural similarities with known mTOR inhibitors, the crystal structure of the mTOR FRB domain complexed with FKBP12 (PDB ID: 3FAP) was used as the receptor for erianin docking. Molecular dynamics simulations provided insights into the stability and dynamics of erianin-receptor complexes over time, which were monitored through root-mean-square deviation (RMSD) values.

Binding free energies (ΔGbind) were predicted using the MM/GBSA approach combined with energy components, including van der Waals, electrostatic, polar, and non-polar interactions. This approach aimed to elucidate binding modes, stability, and energetic attributes of erianin interactions with EPHB2, KDM1A, and mTOR. The binding conformations and the binding conformation pockets were visually represented (**Figure 2E**), accompanied by binding energy computations. EPHB2 and mTOR had the highest docking scores (-8.238 kcal/mol and −8.233 kcal/mol, respectively), followed by KDM1A with a score of −7.479 kcal/mol (**Table 1**). To substantiate these findings, extended five nanosecond molecular dynamics simulations[29] were executed, which refined energy levels and permitting evaluation of interaction energies (**Figure 2F**). The interaction energies of different targets were calculated after the molecular dynamic simulations. A lower ΔGcal value (ΔGcal = ΔEvdw + ΔEele + ΔGpol + ΔGnonpol) is indicative of more favorable binding with a ΔGcal of −29.71, −29.51, and −19.72 for EPHB2, mTOR, and KDM1A, respectively (**Table 2**), suggesting the high potential of EPHB2 and mTOR as targets of erianin in lung cancer cells. Furthermore, the results of the cellular thermal shift assays (CETSA) demonstrated that erianin enhanced the thermotolerance of mTOR (**Figure 2G**), suggesting the potential interaction between erianin and mTOR. Previous studies have demonstrated that mTOR-mediated phosphorylation activates S6K, leading to the activation of CAD and subsequent promotion of *de novo* pyrimidine synthesis[17,18]. Given the significant disruption of pyrimidine metabolism by erianin observed in our combined transcriptome and metabolomics analyses, mTOR emerged as a compelling candidate for erianin intervention in lung cancer cells. We therefore concentrated on mTOR in the subsequent analysis. Additionally, data from the Oncomine database revealed a significant upregulation of mTOR in lung adenocarcinoma (P = 6.91E-4) and lung squamous cell carcinoma (P = 0.042; **Figure 2H**). Further examination of mTOR expression across different stages of lung adenocarcinoma and squamous cell carcinoma development using the UALCAN database demonstrated consistent upregulation of mTOR expression throughout various stages of cancer progression (**Figure 2I**). To validate these findings at the protein level, mTOR protein expression was analyzed in normal and cancerous lung tissues using the HPA database, which provided immunohistochemistry-based protein expression data. The results confirmed that mTOR is overexpressed in lung cancer tissues compared to adjacent normal tissues (**Figure 2J**), highlighting the potential role of mTOR in lung cancer progression and the potential as a therapeutic target. Furthermore, western blot analysis showed that erianin suppresses mTOR activation in lung cancer cells along with mTOR downstream effectors (S6K and CAD; **Figure 2K**). Erianin reduced the levels of p-S6K and p-CAD in H460 lung cancer cells. A similar suppression was also observed when cells were treated with the mTOR inhibitor, rapamycin.

Table 1 Docking score and binding affinity between erianin and the predicted targets

	EPHB2	mTOR	KDM1A
Docking sore (kcal/mol)	−8.238	−8.233	−7.479
Predicted binding affinity (μM)	1.54	1.55	5.92

Table 2 Molecular dynamics simulations energy score of each predicted target

Targets	ΔEele	ΔEvdw	ΔGnonpol	ΔGpol	ΔGcal
EPHB2	−10.32	−39.8	−5.45	25.86	−29.71
mTOR	−14.87	−41.63	−5.99	32.98	−29.51
KDM1A	−13.58	−29.97	−4.33	28.16	−19.72

ΔGcal = ΔEvdw + ΔEele + ΔGpol + ΔGnonpol; ΔEvdw represents Van der Waals force; ΔEele represents electrostatic interaction; ΔGpol represents polar solvent interaction energy; and ΔGnonpol represents non-polar solvent interaction energy.

Overexpression of mTOR counteracted the inhibitory effects of erianin in lung cancer cells

Given the significant downregulation of mTOR phosphorylation by erianin in lung cancer cells, the role of mTOR expression in modulating the inhibitory effects of erianin on cell proliferation was investigated. Specifically, the effect of 3BDO, an activator of mTOR, on the erianin-induced inhibition of cell viability was determined using the CCK-8 assay. The addition of 3BDO partially antagonized the suppressive effect of erianin on cell viability (**Figure S1**), suggesting that mTOR has a role in mediating inhibition of cell viability induced by erianin in lung cancer cells. Furthermore, mTOR was overexpressed in H460 and H1299 cells using an mTOR plasmid (**Figure 3A**). To assess the impact of mTOR overexpression on cell proliferation and the inhibitory effects of erianin on cell growth, the cells were treated with 100 nM erianin for 24 h

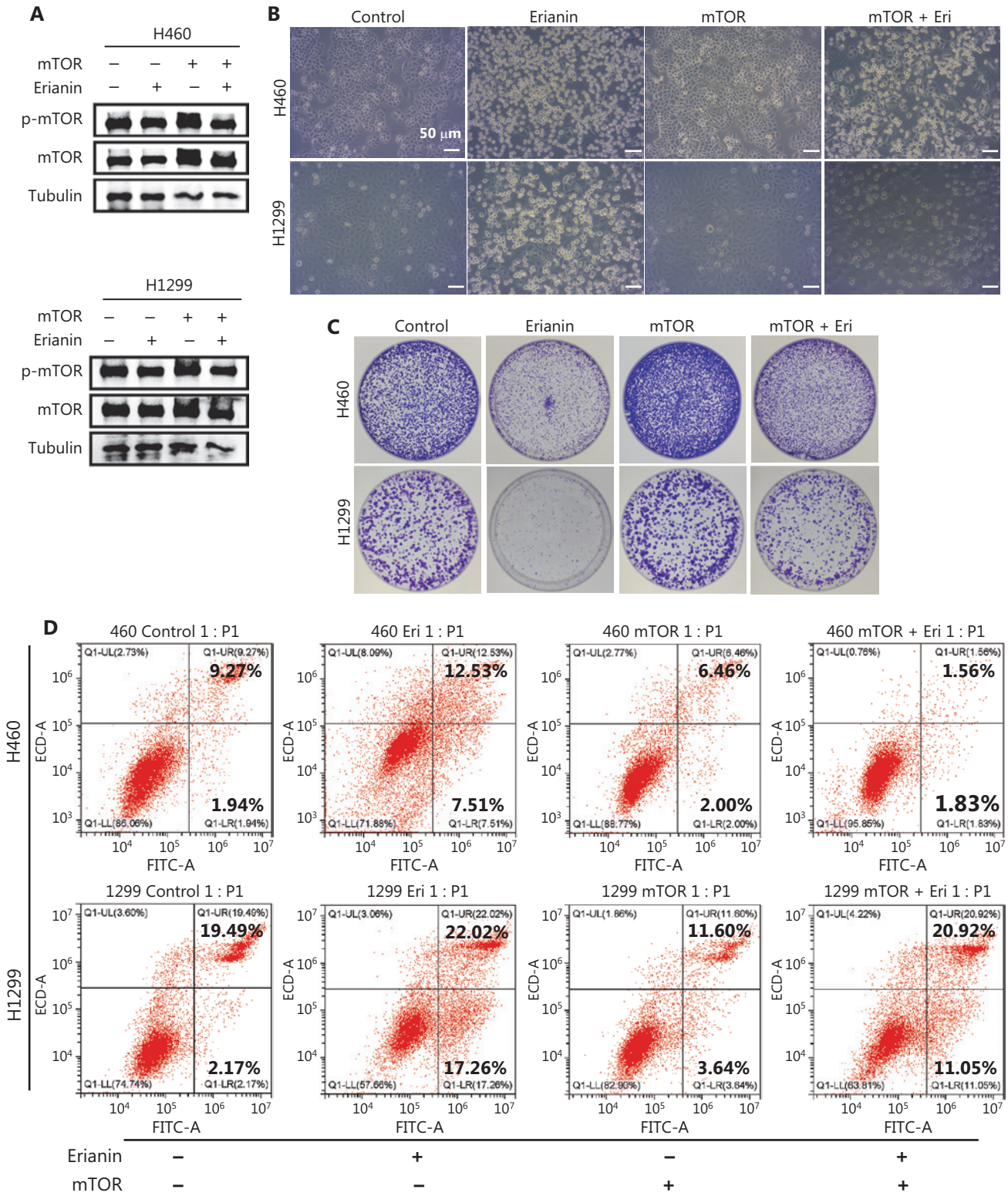

Figure 3 Continued

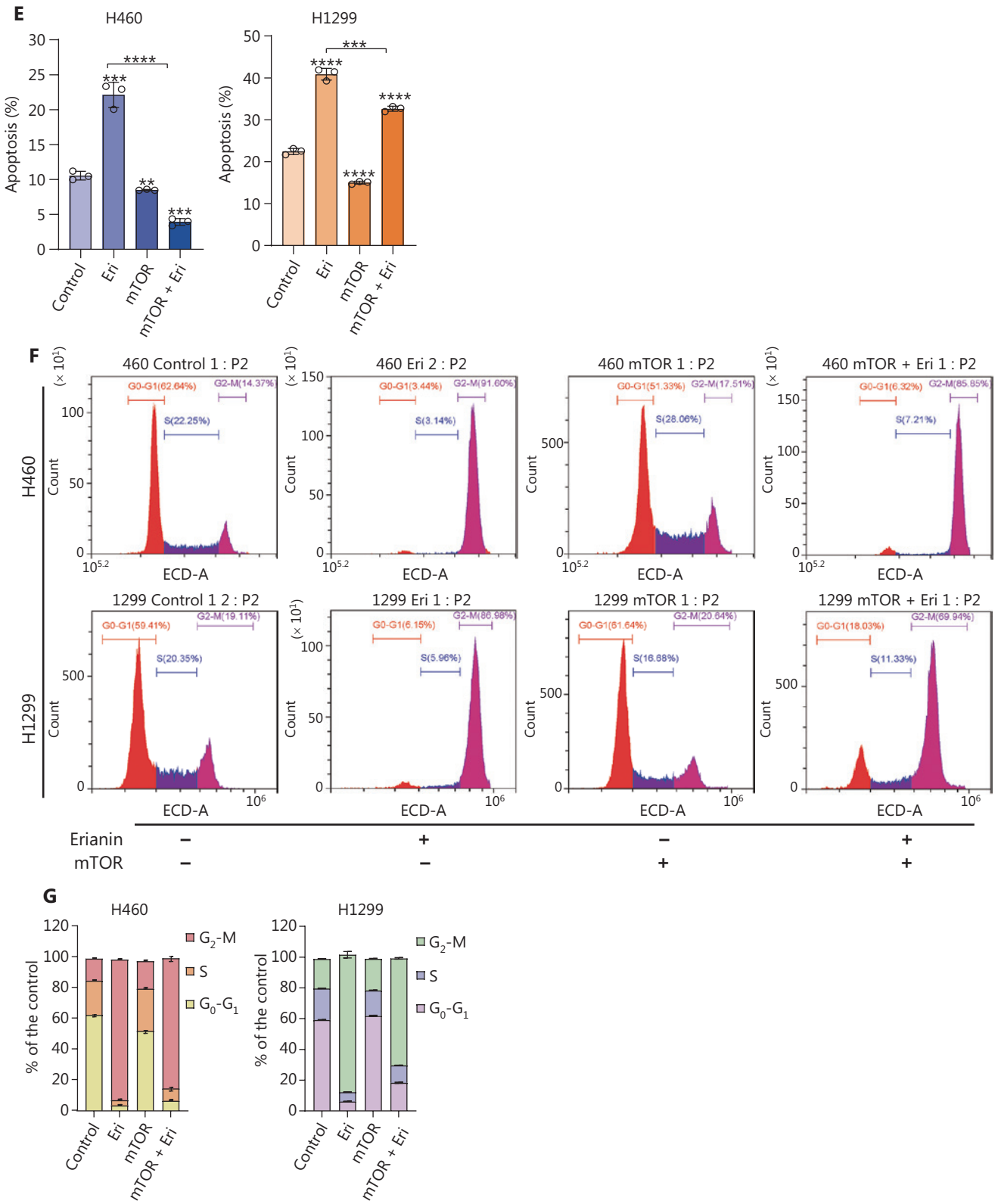

Figure 3 Overexpression of mTOR counteracts the inhibitory effects of erianin in lung cancer cells. (A) Western blot analysis of p-mTOR and mTOR after overexpression of mTOR in H460 and H1299 cells with or without erianin treatment (100 nM). (B) Representative morphologic features of H460 and H1299 cells treated with 100 nM erianin with or without mTOR overexpression; scale bar: 50 μm. (C) Colony formation

of H460 and H1299 cells treated with 100 nM erianin with or without mTOR overexpression. (D) Representative cell apoptosis results determined by flow cytometry after treatment with 100 nM erianin with or without mTOR overexpression in H460 and H1299 cells. (E) Quantitative presentation of cell apoptosis determined by flow cytometry after treatment with 100 nM erianin with or without mTOR overexpression in H460 and H1299 cells; mean ± SD, n = 3, $^{**}P < 0.01$, $^{***}P < 0.001$, $^{****}P < 0.0001$. (F) Representative cell cycle distribution determined by flow cytometry after treatment with 100 nM erianin with or without mTOR overexpression in H460 and H1299 cells. (G) Quantitative presentation of cell cycle distribution determined by flow cytometry after treatment with 100 nM erianin with or without mTOR overexpression in H460 and H1299 cells. The data are presented as the mean ± SD, n = 3.

with or without mTOR overexpression. Microscopic observations indicated that mTOR overexpression reduced cell inhibition induced by erianin treatment (**Figure 3B, Figure S2**). Subsequent colony formation assays demonstrated that mTOR overexpression significantly enhanced cellular proliferation and conferred protection against erianin-induced inhibition of cell growth in H460 and H1299 cell lines (**Figure 3C**). Additionally, an apoptosis assay revealed that erianin treatment significantly increased the percentage of apoptotic cells in both H460 and H1299 cells compared to the control groups (**Figure 3D, E**). However, mTOR overexpression mitigated the apoptotic effect induced by erianin, leading to a reduction in the percentage of apoptotic cells in both cell lines (**Figure 3D, E**). Furthermore, cell cycle analysis showed that erianin treatment caused G_2/M phase cell cycle arrest with approximately 90% of H460 and H1299 cells arrested in the G_2/M phase. Overexpression of mTOR counteracted this effect, reducing the extent of G_2/M phase arrest in both cell lines (**Figure 3F, G**). These findings suggest that mTOR has a critical role in modulating erianin-induced growth inhibition in lung cancer cells.

Knockdown of CAD enhanced the inhibitory effects of erianin in lung cancer cells

To further elucidate the role of erianin-induced downregulation of mTOR activation and the mTOR downstream pivotal pyrimidine metabolism factor, CAD, in mediating erianin-induced cell growth inhibition in lung cancer cells, CAD knockdown experiments were performed. Western blot analysis confirmed CAD knockdown in protein expression (**Figure 4A**). Subsequent microscopic observations (**Figure 4B**) and colony formation assays (**Figure 4C**) revealed that CAD knockdown in H460 and H1299 cells attenuated cellular proliferation and reduced the number of colonies formed. Importantly, CAD knockdown enhanced the induction of cell death and amplified the inhibition of colony formation by erianin in H460 and H1299 cells (**Figure 4B, C**). Furthermore, CAD knockdown intensified the apoptosis induction and G_2/M phase cell cycle arrest effects of erianin in lung cancer cells. A significant increase in the percentage of apoptotic cells (**Figure 4D, E**) and a greater extent of G_2/M phase cell cycle arrest (**Figure 4F, G**) was observed in CAD knockdown H460 and H1299 cells compared to cells treated with erianin alone. Downregulation of CAD activation induced by erianin may impair *de novo* pyrimidine synthesis, resulting in growth inhibition in lung cancer cells. This disruption supports the observation of altered pyrimidine metabolism in erianin-treated lung cancer cells.

Exogenous supplementation of uridine antagonizes the inhibitory effects of erianin in lung cancer cells

Given the significant perturbations in pyrimidine metabolism and downregulation of the mTOR-S6K-CAD signaling axis induced by erianin treatment in lung cancer cells, *in vitro* experiments were performed to determine if the growth inhibition caused by erianin could be rescued by supplementing exogenous pyrimidines and the synthesis substrates. Remarkably, the addition of exogenous uridine was shown to reduce erianin-induced apoptosis in lung cancer cells (**Figure 5A, B**). This finding provides compelling evidence that disruptions in pyrimidine metabolism are integral to the erianin' anticancer mechanism. Additionally, supplementation with exogenous aspartate, a key precursor in pyrimidine biosynthesis, produced effects, especially in H460 cells (**Figure 5C, D**). This finding suggests that the anticancer activity of erianin may, at least in part, be attributed to the ability to impede *de novo* pyrimidine synthesis. Experiments to assess the impact of uridine and aspartate supplementation on the cell cycle arrest induced by erianin were performed in

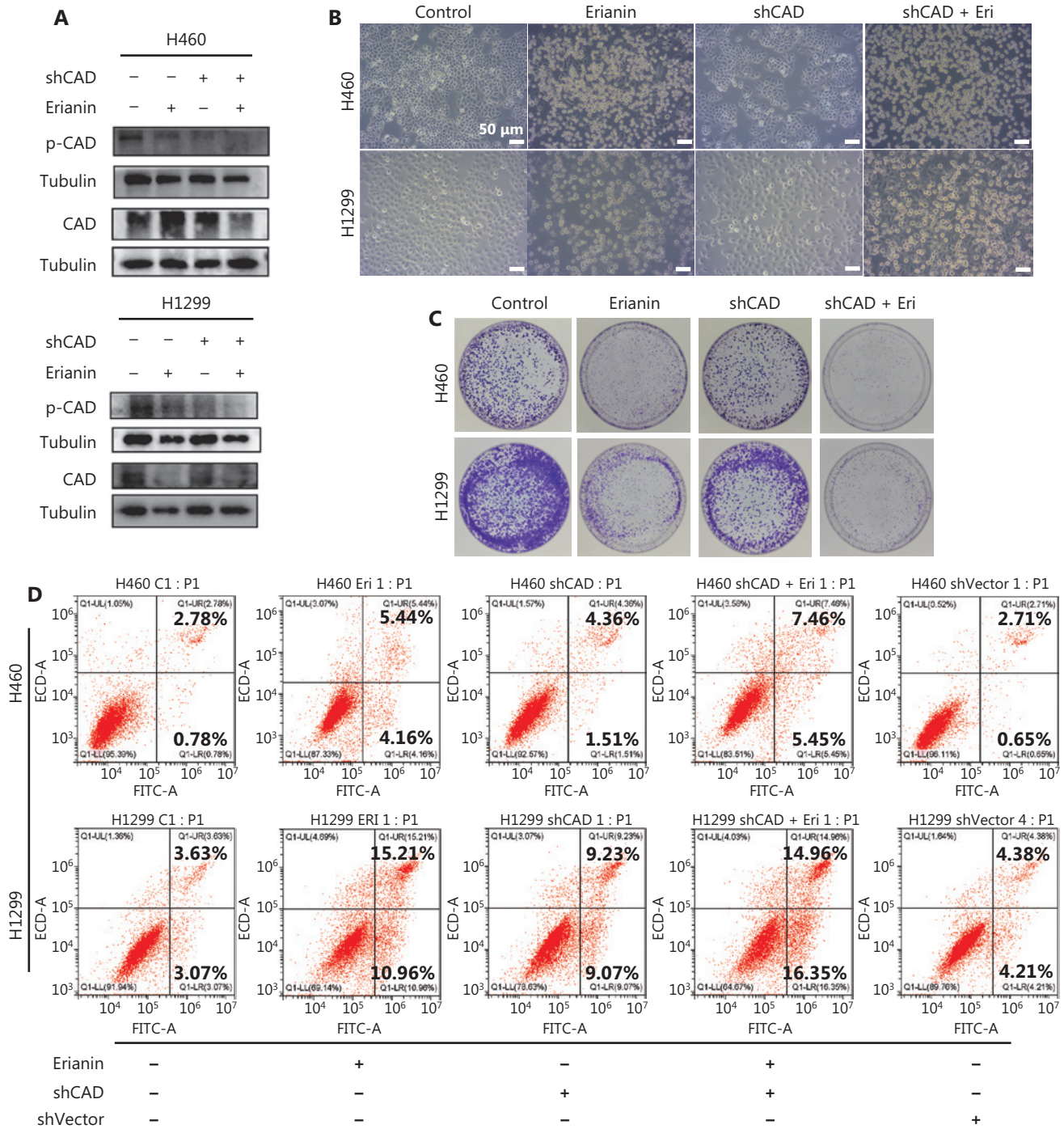

Figure 4 Continued

these cell lines. The addition of uridine partially antagonized the effect of erianin on cell cycle distribution, while supplementation with aspartate did not show a significant effect on cell cycle arrest (**Figure 5E, F**). It is possible that the exogenous addition of uridine typically exerts effects within a shorter time frame because uridine directly participates in the synthesis of pyrimidine nucleotides and influences RNA synthesis within the cell. In contrast, aspartate, as a precursor in pyrimidine biosynthesis, requires conversion through metabolic pathways to form carbamoylglutamate, which subsequently contributes

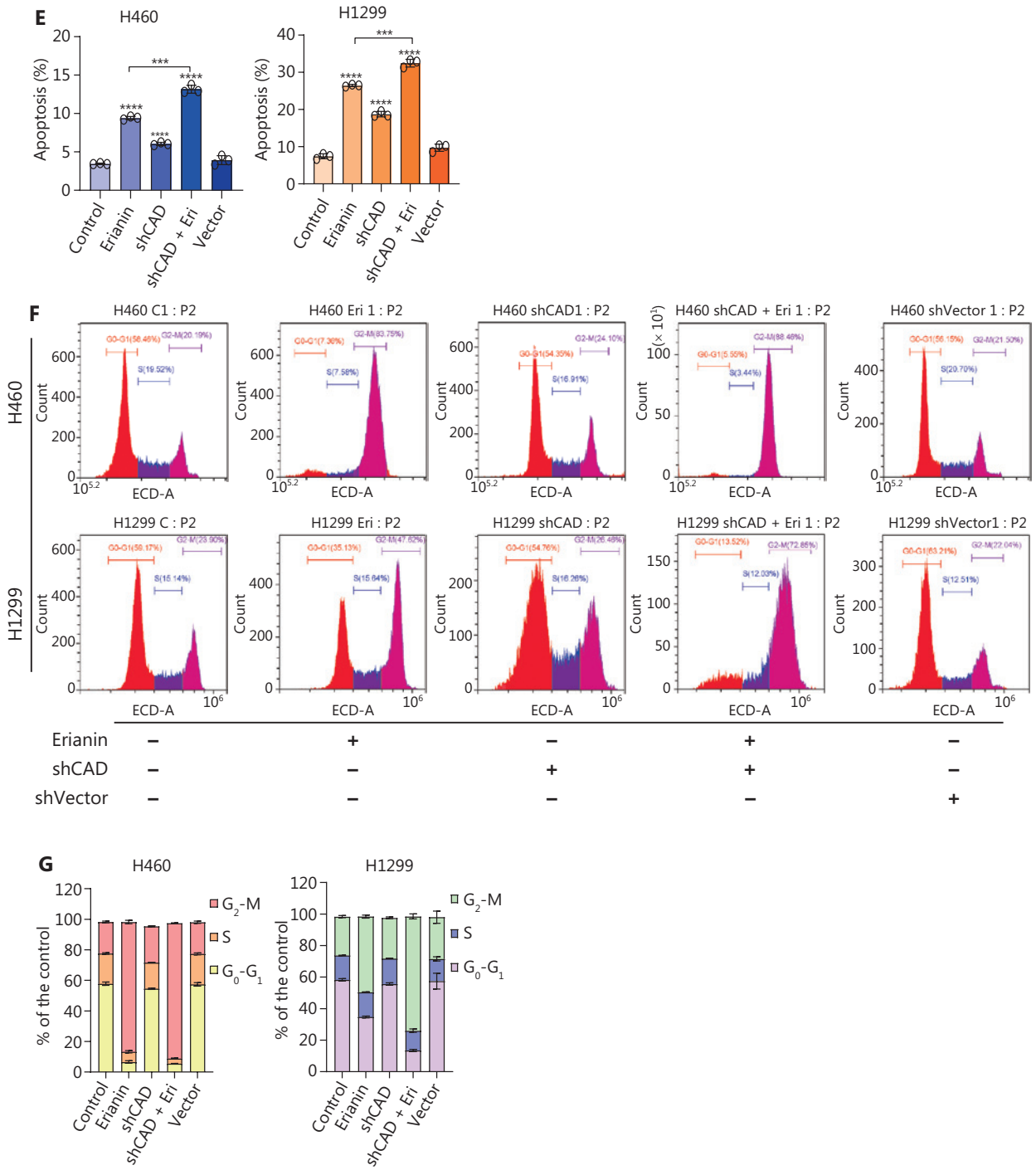

Figure 4 Knockdown of CAD affects cell growth and enhances inhibitory effects of erianin on lung cancer cells. (A) Western blot analysis showing CAD expression following CAD knock-down in H460 and H1299 cells using shRNA-CAD. (B) Representative morphologic images of H460 and H1299 cells treated with erianin (100 nM) with or without CAD knockdown; scale bar: 50 μm. (C) Colony formation of H460 and H1299 cells with erianin treatment (100 nM) with or without CAD knockdown. (D) Representative results of cell apoptosis determined by flow cytometry in H460 and H1299 cells treated with erianin (100 nM) for 24 h with or without CAD knockdown. (E) Quantitative presentation of cell apoptosis determined by flow cytometry in H460 and H1299 cells treated with erianin (100 nM) for 24 h with or without CAD knock-down; mean ± SD, $n = 3$, ***$P < 0.001$, ****$P < 0.0001$. (F) Representative cell cycle distribution determined by flow cytometry in H460 and H1299 cells treated with erianin (100 nM) for 24 h with or without CAD knockdown. (G) Quantitative presentation of cell cycle distribution results determined by flow cytometry in H460 and H1299 cells treated with erianin (100 nM) for 24 h with or without CAD knockdown; mean ± SD, $n = 3$.

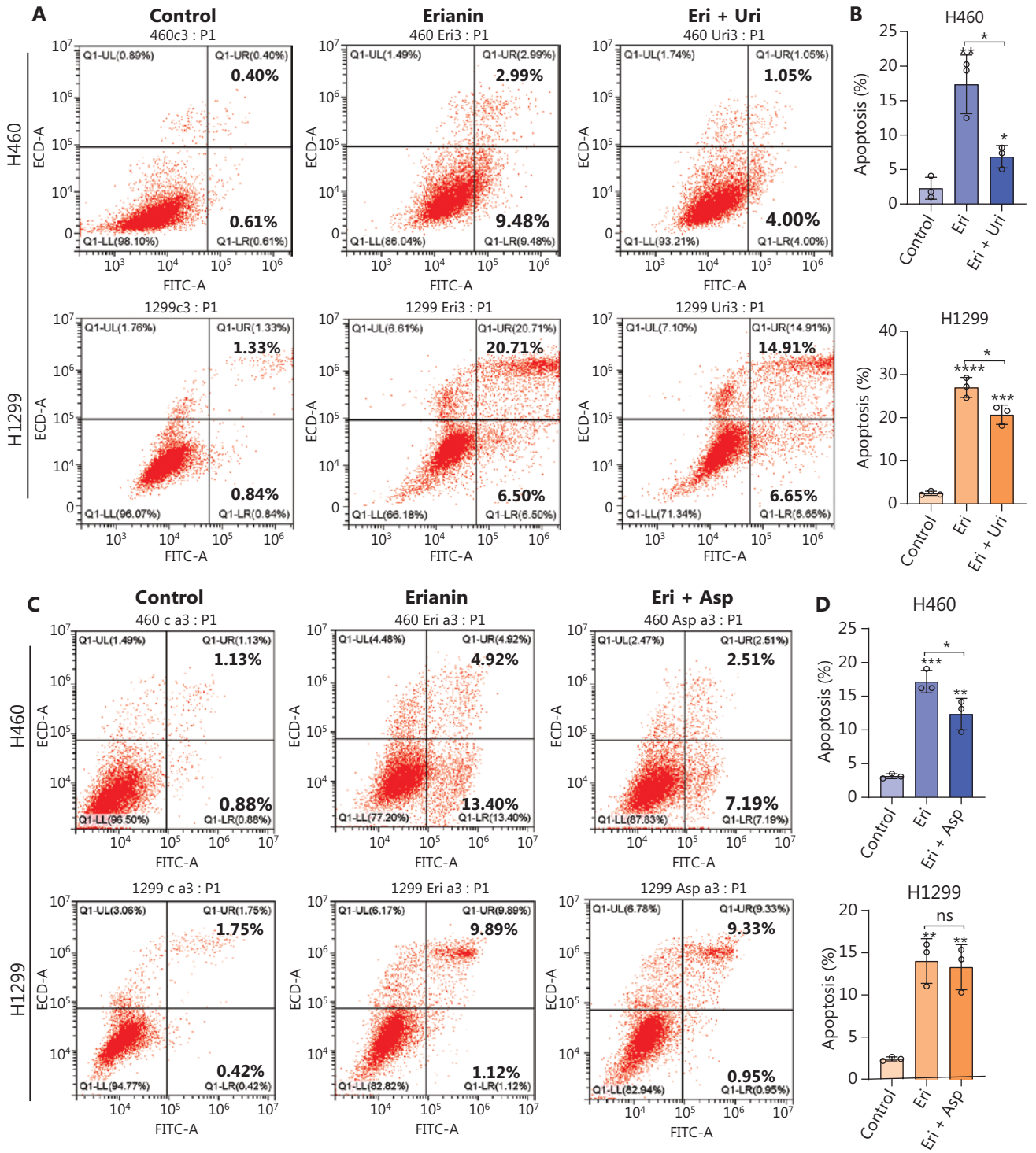

Figure 5 Continued

to the synthesis of uridine monophosphate (UMP) and other pyrimidine nucleotides. Therefore, the exogenous supplementation of aspartate necessitates a more prolonged metabolic process to be converted into active pyrimidine nucleotides. Consequently, the effects of uridine supplementation may work more rapidly than aspartate.

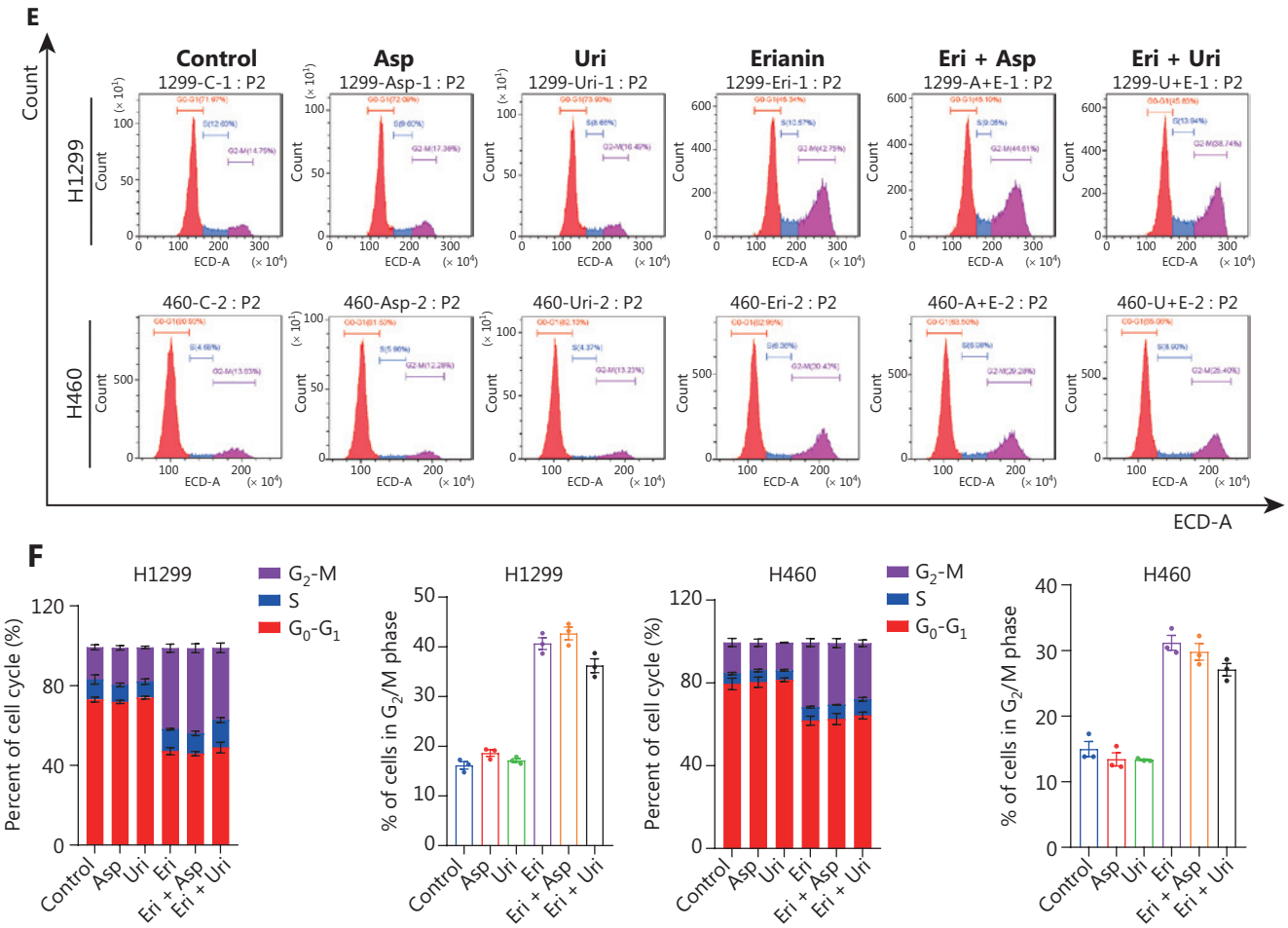

Figure 5 The impact of exogenous uridine and aspartate supplementation on the inhibitory effects of erianin in lung cancer cells. (A) Flow cytometry analysis of cell apoptosis following treatment with erianin (100 nM) with or without exogenous uridine supplementation (100 μM). (B) Quantitative data of cell apoptosis following treatment with erianin (100 nM) with or without exogenous uridine supplementation (100 μM) in H460 and H1299 cells are presented as the mean ± SD, n = 3, *P < 0.05, **P < 0.01, ***P < 0.001, ****P < 0.0001. (C) Flow cytometry analysis of cell apoptosis following treatment with erianin (100 nM) with or without exogenous aspartate supplementation (2 mM). (D) Quantitative data of cell apoptosis following treatment with erianin (100 nM) with or without exogenous aspartate supplementation (2 mM) in H460 and H1299 cells are presented as the mean ± SD, n = 3, ns: no significance, *P < 0.05, **P < 0.01, ***P < 0.001. (E) Flow cytometry analysis of cell cycle distribution following treatment with erianin with or without exogenous aspartate or uridine supplementation in H460 and H1299 cells. (F) Quantitative analysis of cell cycle distribution following treatment with erianin with or without exogenous aspartate or uridine supplementation in H460 and H1299 cells; mean ± SD, n = 3.

Erianin inhibited lung cancer cell growth *in vivo*

To evaluate the inhibitory effects of erianin on lung cancer through downregulation of mTOR activation and disruption of pyrimidine metabolism *in vivo*, a subcutaneous xenograft model was established using H460 cells. Once the xenografts reached approximately 70 mm^3 in size, the mice were randomly divided into the following 4 groups: low-dose erianin (50 mg/kg); medium-dose erianin (100 mg/kg); high-dose erianin (200 mg/kg); and a control group. Parameters, such as body weight and tumor volume, were measured every other day to assess treatment effects. As shown in **Figure 6A-C**, intraperitoneal administration of medium and high doses of erianin resulted in significant inhibition of tumor growth compared to the control group. There was no significant difference in the

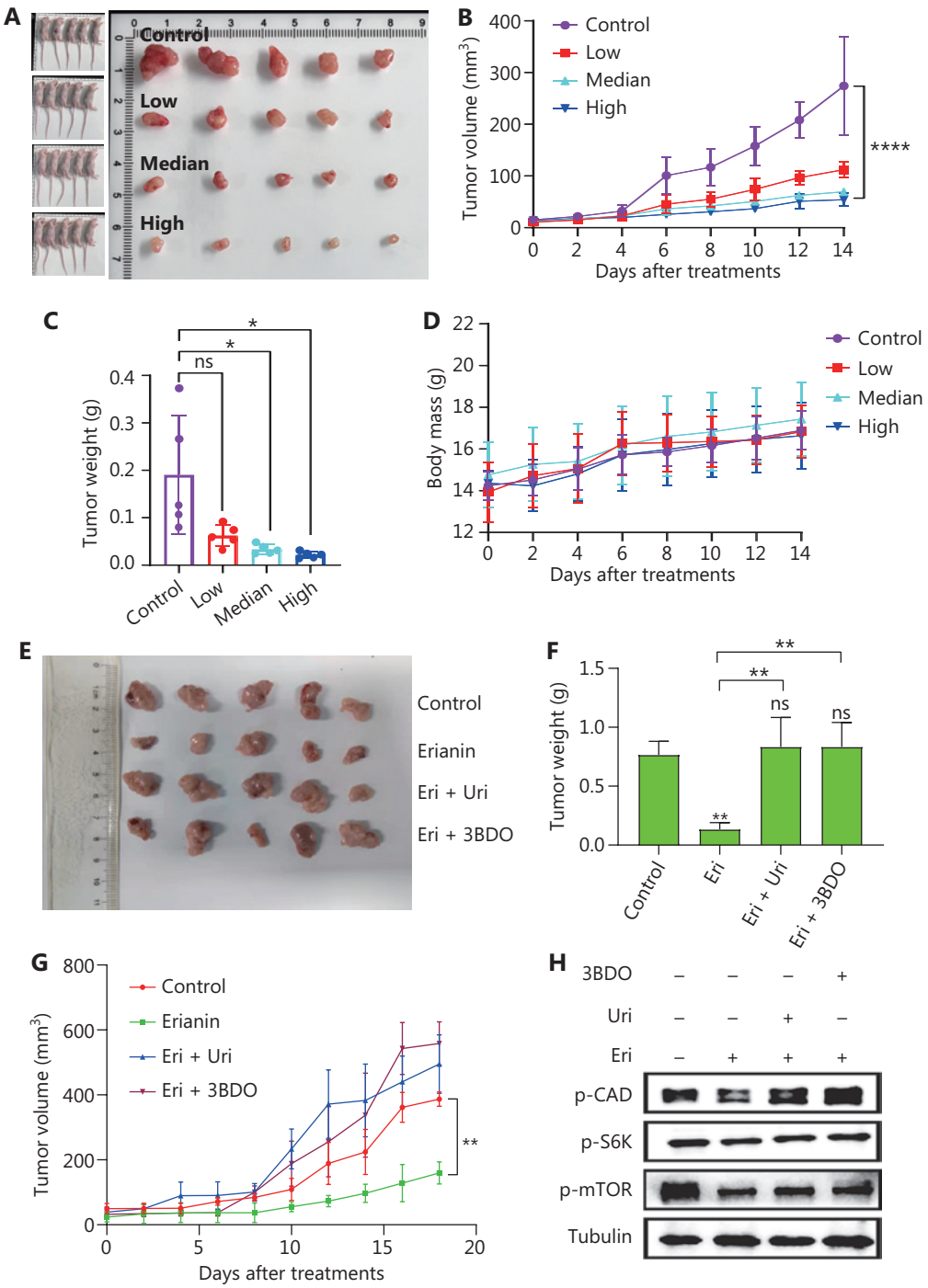

Figure 6 Evaluation of the inhibitory effects of erianin on lung cancer *in vivo*. (A) Tumor images of H460 xenograft tumors following treatment with different doses of erianin. (B) Tumor volume changes of H460 xenograft tumors following treatment with different doses of erianin; mean ± SD, $n = 5$, ****$P < 0.0001$. (C) Tumor weights of H460 xenograft tumors following treatment with different doses of erianin; mean ± SD, $n = 5$, ns, not significant, *$P < 0.05$. (D) Body mass changes of mice following treatment with different doses of erianin; mean ± SD, $n = 5$. (E) Tumor images of H460 xenograft tumors after erianin treatment (100 mg/kg) with or without uridine/3BDO supplementation. (F) Tumor weights of H460 xenograft tumors after erianin treatment (100 mg/kg) with or without uridine/3BDO supplementation; mean + SD, $n = 5$, ns: no significance, **$P < 0.01$. (G) Tumor volumes of H460 xenograft tumors following erianin treatment (100 mg/kg) with or without uridine (33.4 g/kg) / 3BDO (0.05 g/kg) supplementation, mean ± SD, $n = 5$, **$P < 0.01$. (H) Western blot analysis of p-mTOR, p-S6K, and p-CAD in tumor tissues obtained from different treatment groups (erianin alone or in combination with uridine or 3BDO).

body weight among the groups (**Figure 6D**). Based on these observations, the medium dose of erianin (100 mg/kg) was selected for subsequent investigations.

To further confirm that erianin inhibits lung cancer cell growth by regulating pyrimidine metabolism and mTOR activation *in vivo*, mice with tumors were divided into the following four groups: erianin; erianin + uridine; erianin + 3BDO (an mTOR activator); and a control group. The erianin group received erianin (100 mg/kg) and the uridine and 3BDO groups were treated with uridine (33.4 g/kg) and 3BDO (0.05 g/kg) in addition to erianin (100 mg/kg). Tumor volume and weight were measured to evaluate the impact of each treatment on lung cancer cell growth. Tumor tissue in each group was photographed at the end of the experiment (**Figure 6E**). Remarkably, co-treatment with erianin and 3BDO or exogenous uridine resulted in increased tumor weight (**Figure 6F**) and volume (**Figure 6G**) compared to erianin treatment alone. This finding suggests that the addition of an mTOR activator or exogenous pyrimidines counteracts the tumor growth-inhibitory effects of erianin *in vivo*.

Furthermore, western blot analysis of tumor tissue revealed reduced levels of p-mTOR, p-S6K, and p-CAD expression in erianin-treated tumors. However, the administration of uridine or 3BDO antagonized the inhibitory effect of erianin on the mTOR-S6K-CAD axis (**Figure 6H**). These results support the notion that erianin effectively inhibits the phosphorylation and activation of mTOR and mTOR downstream factors (S6K and CAD) *in vivo*. This finding further validates the relevance of the mTOR-related signaling pathway and pyrimidine metabolism in the erianin anticancer effects, suggesting that the therapeutic potential of erianin in lung cancer may be, at least in part, mediated through modulation of pyrimidine metabolism *via* suppression of mTOR activation.

Discussion

Lung cancer represents a significant health burden in China[30], underscoring the urgent need for innovative therapeutic strategies. Traditionally, platinum-based chemotherapy has been the standard treatment for advanced stages of lung cancer. However, the efficacy of platinum-based chemotherapy is often compromised by primary or secondary drug resistance and severe adverse effects[8]. These challenges contribute to a relatively low overall cure rate among patients. Natural products derived from plants, animals, microorganisms, and marine sources have emerged as valuable sources of bioactive compounds with potential applications in cancer therapy[31-35]. These compounds influence various cellular processes involved in cancer progression, including cell proliferation, apoptosis, ferroptosis, autophagy, and angiogenesis[36-40]. Erianin, a natural compound extracted from the traditional Chinese medicinal plant, *Dendrobium chrysotoxum* Lindl., has demonstrated promising anticancer activity, especially against lung cancer[12]. The natural compound, erianin, from TCM has shown significant advantages in anti-tumor activity due to its multi-target effects, modulation of immune responses, reduction of chemotherapy side effects, low toxicity, and high safety profile. Erianin enhances the chemotherapy sensitivity of lung cancer cells and may serve as a valuable adjuvant in lung cancer chemotherapy[41]. Additionally, erianin significantly inhibits the proliferation of oxaliplatin-resistant human colon cancer cells, providing a theoretical basis for its clinical application in platinum-based chemotherapy for colon cancer[42]. In the current study evidence was provided that erianin effectively inhibits lung cancer cell growth both *in vitro* and *in vivo*, highlighting its significant anti-lung cancer effects. Through the integration of transcriptomic and metabolomic analyses, the results herein suggest that erianin affects pyrimidine metabolism in lung cancer cells, potentially by inhibiting activation of the mTOR-related signaling pathway.

Omics techniques are extensively used in cancer research, providing a comprehensive evaluation of molecular entities. To elucidate the molecular effects of erianin in greater detail, mRNA sequencing and non-targeted metabolomics analyses were performed on lung cancer cells treated with erianin along with untreated controls. The results revealed significant alterations in pyrimidine metabolism in the erianin-treated lung cancer cells, as evidenced by differential gene expression and metabolite profiles between the treated and untreated groups. Metabolic alterations are characteristic of cancer cells[43] and the synthesis and utilization of nucleotides represent a crucial metabolic dependency across various cancer types[44,45]. Recent research has established a link between genes involved in pyrimidine metabolism and cancer progression, suggesting that targeting key enzymes and pathways within this metabolism could exert anticancer effects by disrupting nucleotide synthesis, inhibiting cellular proliferation, and promoting apoptosis[13,46-48]. Given the observed changes in pyrimidine metabolism in

erianin-treated lung cancer cells, we hypothesized that erianin may exert its effects, at least in part, by modulating nucleotide metabolism (especially pyrimidine biosynthesis). To further investigate this hypothesis, lung cancer cells treated with erianin were supplemented with exogenous uridine and its biosynthesis precursor, aspartate. The results indicated that supplementation with exogenous uridine mitigated the inhibitory effects of erianin on lung cancer cells, supporting our hypothesis that alterations in pyrimidine metabolism contribute to the erianin-mediated inhibition of lung cancer cell growth. Our previous studies have shown that erianin promotes ferroptosis[12]. It has been reported that a multi-enzyme complex involved in *de novo* pyrimidine synthesis is termed "pyrimidinosome." Activated AMP-activated protein kinase enhances the assembly of "pyrimidinosome," thereby promoting DHODH-mediated ferroptosis defense[46]. These findings suggest a potential link between pyrimidine metabolism and ferroptosis, indicating that targeting pyrimidine metabolic pathways may also facilitate the induction of ferroptosis in cancer cells.

mTOR is an evolutionarily conserved serine/threonine kinase that primarily regulates cell growth and metabolism[49]. Network pharmacology analysis has identified mTOR as a potential target of erianin in lung cancer. This robust approach enables the investigation of drug-cell interactions and regulatory mechanisms[50,51], facilitating exploration of the anticancer effects of natural products. Molecular docking studies suggest that erianin may bind to mTOR, a prediction that was validated by western blot analysis which demonstrated that erianin downregulates mTOR phosphorylation in lung cancer cells. Previous research by Zhang et al.[52] established that erianin inhibits lung cancer cell proliferation *via* the PI3K/AKT/mTOR signaling pathway, underscoring the influence on mTOR-related signaling. However, further investigation is needed to clarify how alterations in mTOR expression affect the inhibitory effects of erianin in lung cancer cells and to elucidate the downstream consequences of mTOR suppression induced by erianin. Moreover, data analysis from the Oncomine, UALCAN, and HPA databases revealed that mTOR expression is significantly elevated in lung cancer tissues compared to healthy controls. This finding highlights the pivotal role of mTOR in promoting cell growth and proliferation in lung cancer, emphasizing the potential of mTOR as a therapeutic target. The literature consistently reports that mTOR activation contributes to tumor progression[53,54], generating significant interest in targeting this aberrant pathway as a therapeutic strategy. Several mTOR inhibitors are currently being developed for cancer therapy[23]. The results herein indicated that erianin reduces mTOR phosphorylation in lung cancer cells. Overexpression of mTOR mitigated the inhibitory effects of erianin on lung cancer cells. These findings substantiate the hypothesis that erianin exerts anti-lung cancer effects through inhibition of mTOR activation. mTOR is a crucial signaling molecule involved in regulating cellular metabolism[55,56]. The initial steps of pyrimidine biosynthesis are governed by CAD, which can be phosphorylated by mTOR through S6K. This phosphorylation process facilitates pyrimidine synthesis and cell cycle progression[18]. Consistent with this process, the current study demonstrated downregulation of S6K and CAD phosphorylation in lung cancer cells treated with erianin. Notably, CAD knockdown enhances the inhibitory effects of erianin on lung cancer cell growth. These findings suggest that erianin disrupts pyrimidine metabolism in lung cancer cells by inhibiting mTOR activation and mTOR downstream targets (S6K and CAD). This disruption likely contributes to the anticancer activity of erianin in lung cancer (**Figure 7**). In contrast, it should be noted that the inhibition of the mTOR signaling pathway by erianin is less pronounced compared to the positive control (rapamycin), as demonstrated by western blot analysis in the current study. While this pathway has a role in the regulatory mechanisms of erianin, the mTOR signaling pathway is unlikely to serve as its primary mode of action. Further exploration of alternative mechanisms of action for erianin, such as other cell death pathways or signaling networks that may contribute to its cytotoxic effects, will be a focus of future research.

Furthermore, it should be noted that erianin has low solubility in water and a rapid metabolism and excretion rate, leading to poor bioavailability, which greatly hinders its clinical application[57]. The development of erianin derivatives in the future may have significant importance. As indicated in our previous study, erianin has poor water solubility but exhibits high intestinal absorption and blood-brain barrier permeability, which are important for the treatment of some tumors. The erianin toxicity levels are also lower than osimertinib and pemetrexed[11]. Due to the notable anti-tumor effects, there have been relevant studies on the synthesis, structural modification, and pharmacologic effects of erianin[58]. These investigations highlight the significant anticancer potential of erianin, warranting further exploration of pharmacologic mechanisms to provide a reference for future applications.

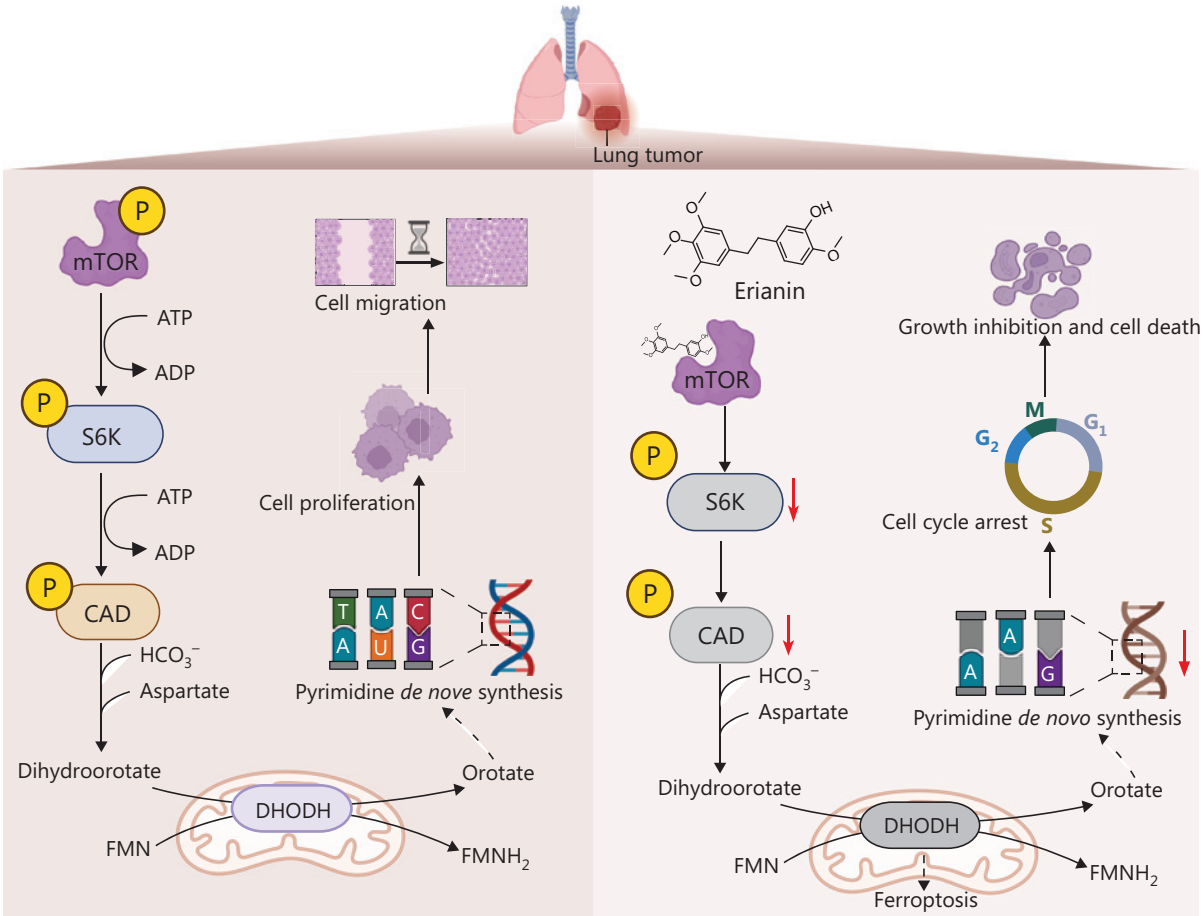

Figure 7 Schematic representation illustrating the mechanism of action of erianin in lung cancer. Pyrimidine biosynthesis, a process essential for DNA and RNA synthesis, has a crucial role in regulating cellular growth. The initial steps of this biosynthetic pathway are catalyzed by the enzyme complex, CAD, comprised of carbamoyl-phosphate synthetase, aspartate transcarbamylase, and dihydroorotase. CAD activation is mediated by the mammalian target of rapamycin (mTOR) through S6K-mediated phosphorylation. This activation promotes pyrimidine biosynthesis and supports cell cycle progression by facilitating the formation of dihydroorotate, the first committed intermediate in the pathway. The early stages of pyrimidine biosynthesis depend on essential substrates, including HCO_3^- (bicarbonate) and aspartate. A critical subsequent step in the pathway involves dihydroorotate dehydrogenase (DHODH), a rate-limiting enzyme that catalyzes the oxidation of dihydroorotate to orotate. This reaction is facilitated by the co-factor, flavin mononucleotide (FMN), which is reduced to $FMNH_2$ as it accepts electrons during the oxidation process. Inhibition of DHODH disrupts pyrimidine metabolism, leading to oxidative stress, nucleotide depletion, and an increased susceptibility to ferroptosis, highlighting a functional link between pyrimidine metabolism and ferroptosis. Erianin was identified as a molecular inhibitor of mTOR signaling in lung cancer. By suppressing mTOR phosphorylation, erianin impairs the activation of downstream effectors, including S6K and CAD. Consequently, erianin disrupts pyrimidine biosynthesis, leading to impaired nucleotide production and the inhibition of cell growth and proliferation. The dashed arrow in the schematic representation indicates that the pathway involves multiple intermediate reactions or multi-step processes, rather than a single direct enzymatic reaction.

Conclusions

In conclusion, our study highlights the notable anticancer effects of erianin in lung cancer. Key factors underlying the therapeutic effects of erianin include modulation of pyrimidine metabolism and suppression of mTOR activation along with the mTOR downstream targets (S6K and CAD). These findings significantly enhance our understanding of the molecular mechanisms driving erianin anticancer properties and provide a robust rationale for further preclinical and

clinical investigations to fully explore the therapeutic potential of erianin in lung cancer treatment.

Grant support

This work was supported by the National Natural Science Foundation of China (82104207) and Natural Science Foundation of Zhejiang Province (LQ22H280001).

Conflict of interest statement

No potential conflicts of interest are disclosed.

Author contributions

Conceived and designed the analysis: Xinbing Sui, Xueni Sun.
Collected the data: Lili Yan, Yanfen Liu, Yufei Huang, Xiaoyu Sun, Haiyang Jiang, Jie Gu, Jing Xia.
Performed the analysis: Lili Yan, Yanfen Liu, Yufei Huang, Xiaoyu Sun, Haiyang Jiang, Jie Gu, Jing Xia.
Wrote the paper: Lili Yan, Yanfen Liu, Xueni Sun.

Data availability statement

The data generated in this study are available upon request from the corresponding author.

References

1. Siegel RL, Giaquinto AN, Jemal A. Cancer statistics, 2024. CA Cancer J Clin. 2024; 74: 12-49.
2. Bray F, Laversanne M, Sung H, Ferlay J, Siegel RL, Soerjomataram I, et al. Global cancer statistics 2022: GLOBOCAN estimates of incidence and mortality worldwide for 36 cancers in 185 countries. CA Cancer J Clin. 2024; 74: 229-63.
3. Maomao C, He L, Dianqin S, Siyi H, Xinxin Y, Fan Y, et al. Current cancer burden in China: epidemiology, etiology, and prevention. Cancer Biol Med. 2022; 19: 1121-38.
4. Thai AA, Solomon BJ, Sequist LV, Gainor JF, Heist RS. Lung cancer. Lancet. 2021; 398: 535-54.
5. Ettinger DS, Wood DE, Aisner DL, Akerley W, Bauman JR, Bharat A, et al. Non-small cell lung cancer, version 3.2022, NCCN clinical practice guidelines in oncology. J Natl Compr Canc Netw. 2022; 20: 497-530.
6. Ettinger DS, Wood DE, Aisner DL, Akerley W, Bauman JR, Bharat A, et al. NCCN guidelines insights: non-small cell lung cancer, version 2.2021. J Natl Compr Canc Netw. 2021; 19: 254-66.
7. Ettinger DS, Wood DE, Aisner DL, Akerley W, Bauman J, Chirieac LR, et al. Non-small cell lung cancer, version 5.2017, NCCN clinical practice guidelines in oncology. J Natl Compr Canc Netw. 2017; 15: 504-35.
8. Griesinger F, Korol EE, Kayaniyil S, Varol N, Ebner T, Goring SM. Efficacy and safety of first-line carboplatin-versus cisplatin-based chemotherapy for non-small cell lung cancer: a meta-analysis. Lung Cancer. 2019; 135: 196-204.
9. Naeem A, Hu P, Yang M, Zhang J, Liu Y, Zhu W, et al. Natural products as anticancer agents: current status and future perspectives. Molecules. 2022; 27: 8367.
10. Yang Y, Li N, Wang TM, Di L. Natural products with activity against lung cancer: a review focusing on the tumor microenvironment. Int J Mol Sci. 2021; 22: 10827.
11. Yan L, Zhang Z, Liu Y, Ren S, Zhu Z, Wei L, et al. Anticancer activity of erianin: cancer-specific target prediction based on network pharmacology. Front Mol Biosci. 2022; 9: 862932.
12. Chen P, Wu Q, Feng J, Yan L, Sun Y, Liu S, et al. Erianin, a novel dibenzyl compound in dendrobium extract, inhibits lung cancer cell growth and migration via calcium/calmodulin-dependent ferroptosis. Signal Transduct Target Ther. 2020; 5: 51.
13. Shi DD, Savani MR, Levitt MM, Wang AC, Endress JE, Bird CE, et al. De novo pyrimidine synthesis is a targetable vulnerability in IDH mutant glioma. Cancer Cell. 2022; 40: 939-56.
14. Brown KK, Spinelli JB, Asara JM, Toker A. Adaptive reprogramming of de novo pyrimidine synthesis is a metabolic vulnerability in triple-negative breast cancer. Cancer Discov. 2017; 7: 391-9.
15. Li G, Li D, Wang T, He S. Pyrimidine biosynthetic enzyme CAD: its function, regulation, and diagnostic potential. Int J Mol Sci. 2021; 22: 10253.
16. Ridder DA, Schindeldecker M, Weinmann A, Berndt K, Urbansky L, Witzel HR, et al. Key enzymes in pyrimidine synthesis, CAD and CPS1, predict prognosis in hepatocellular carcinoma. Cancers (Basel). 2021; 13: 744.
17. Robitaille AM, Christen S, Shimobayashi M, Cornu M, Fava LL, Moes S, et al. Quantitative phosphoproteomics reveal mTORC1 activates de novo pyrimidine synthesis. Science. 2013; 339: 1320-3.
18. Ben-Sahra I, Howell JJ, Asara JM, Manning BD. Stimulation of de novo pyrimidine synthesis by growth signaling through mTOR and S6K1. Science. 2013; 339: 1323-8.
19. Mir SA, Dar A, Alshehri SA, Wahab S, Hamid L, Almoyad MAA, et al. Exploring the mTOR signalling pathway and its inhibitory scope in cancer. Pharmaceuticals (Basel). 2023; 16: 1004.
20. Zhang H, Su X, Burley SK, Zheng XFS. mTOR regulates aerobic glycolysis through NEAT1 and nuclear paraspeckle-mediated mechanism in hepatocellular carcinoma. Theranostics. 2022; 12: 3518-33.
21. Murugan AK. mTOR: role in cancer, metastasis and drug resistance. Semin Cancer Biol. 2019; 59: 92-111.
22. Hua H, Kong Q, Zhang H, Wang J, Luo T, Jiang Y. Targeting mTOR for cancer therapy. J Hematol Oncol. 2019; 12: 71.

23. Mao B, Zhang Q, Ma L, Zhao DS, Zhao P, Yan P. Overview of research into mTOR inhibitors. Molecules. 2022; 27: 5295.
24. Duchatel RJ, Jackson ER, Parackal SG, Kiltschewskij D, Findlay IJ, Mannan A, et al. PI3k/mTOR is a therapeutically targetable genetic dependency in diffuse intrinsic pontine glioma. J Clin Invest. 2024; 134: e170329.
25. Browne IM, André F, Chandarlapaty S, Carey LA, Turner NC. Optimal targeting of PI3K-AKT and mTOR in advanced oestrogen receptor-positive breast cancer. Lancet Oncol. 2024; 25: e139-51.
26. Korfel A, Schlegel U, Herrlinger U, Dreyling M, Schmidt C, von Baumgarten L, et al. Phase II trial of temsirolimus for relapsed/refractory primary CNS lymphoma. J Clin Oncol. 2016; 34: 1757-63.
27. Haas-Kogan DA, Aboian MS, Minturn JE, Leary SES, Abdelbaki MS, Goldman S, et al. Everolimus for children with recurrent or progressive low-grade glioma: results from the phase II PNOC001 trial. J Clin Oncol. 2024; 42: 441-51.
28. Yao JC, Pavel M, Lombard-Bohas C, Van Cutsem E, Voi M, Brandt U, et al. Everolimus for the treatment of advanced pancreatic neuroendocrine tumors: overall survival and circulating biomarkers from the randomized, phase III RADIANT-3 study. J Clin Oncol. 2016; 34: 3906-13.
29. Śledź P, Caflisch A. Protein structure-based drug design: from docking to molecular dynamics. Curr Opin Struct Biol. 2018; 48: 93-102.
30. Qi J, Li M, Wang L, Hu Y, Liu W, Long Z, et al. National and subnational trends in cancer burden in China, 2005-20: an analysis of national mortality surveillance data. Lancet Public Health. 2023; 8: e943-55.
31. Wang Y, Li J, Xia L. Plant-derived natural products and combination therapy in liver cancer. Front Oncol. 2023; 13: 1116532.
32. Park SY, Choi H, Chung JW. Reptiles as promising sources of medicinal natural products for cancer therapeutic drugs. Pharmaceutics. 2022; 14: 874.
33. Khalifa SAM, Elias N, Farag MA, Chen L, Saeed A, Hegazy MF, et al. Marine natural products: a source of novel anticancer drugs. Mar Drugs. 2019; 17: 491.
34. Duffy R, Wade C, Chang R. Discovery of anticancer drugs from antimalarial natural products: a MEDLINE literature review. Drug Discov Today. 2012; 17: 942-53.
35. Huang M, Liu C, Shao Y, Zhou S, Hu G, Yin S, et al. Anti-tumor pharmacology of natural products targeting mitosis. Cancer Biol Med. 2022; 19: 774-801.
36. Guo Z, Wang S, Hao H, Deng X, Fu J, Guo Y, et al. Targeting ferroptosis in cancer by natural products: an updated review. Am J Chin Med. 2023; 51: 547-74.
37. Ai Y, Zhao Z, Wang H, Zhang X, Qin W, Guo Y, et al. Pull the plug: anti-angiogenesis potential of natural products in gastrointestinal cancer therapy. Phytother Res. 2022; 36: 3371-93.
38. Rajabi S, Maresca M, Yumashev AV, Choopani R, Hajimehdipoor H. The most competent plant-derived natural products for targeting apoptosis in cancer therapy. Biomolecules. 2021; 11: 534.
39. Fontana F, Raimondi M, Marzagalli M, Di Domizio A, Limonta P. The emerging role of paraptosis in tumor cell biology: perspectives for cancer prevention and therapy with natural compounds. Biochim Biophys Acta Rev Cancer. 2020; 1873: 188338.
40. Zhou X, Yue GG, Tsui SK, Pu J, Fung KP, Lau CB. Elaborating the role of natural products on the regulation of autophagy and their potentials in breast cancer therapy. Curr Cancer Drug Tartets. 2018; 18: 239-55.
41. Lv J, Wang Z, Liu H. Erianin suppressed lung cancer stemness and chemotherapeutic sensitivity via triggering ferroptosis. Environ Toxicol. 2024; 39: 479-86.
42. Su C, Liu S, Ma X, Liu J, Liu J, Lei M, et al. The effect and mechanism of erianin on the reversal of oxaliplatin resistance in human colon cancer cells. Cell Biol Int. 2021; 45: 2420-8.
43. Pavlova NN, Thompson CB. The emerging hallmarks of cancer metabolism. Cell Metab. 2016; 23: 27-47.
44. Mullen NJ, Singh PK. Nucleotide metabolism: a pan-cancer metabolic dependency. Nat Rev Cancer. 2023; 23: 275-94.
45. Shi DD, Savani MR, Abdullah KG, McBrayer SK. Emerging roles of nucleotide metabolism in cancer. Trends Cancer. 2023; 9: 624-35.
46. Yang C, Zhao Y, Wang L, Guo Z, Ma L, Yang R, et al. De novo pyrimidine biosynthetic complexes support cancer cell proliferation and ferroptosis defence. Nat Cell Biol. 2023; 25: 836-47.
47. Backer N, Kumar A, Singh AK, Singh H, Narasimhan B, Kumar P. Medicinal chemistry aspects of uracil containing dUTPase inhibitors targeting colorectal cancer. Drug Discov Today. 2023; 29: 103853.
48. Wang W, Cui J, Ma H, Lu W, Huang J. Targeting pyrimidine metabolism in the era of precision cancer medicine. Front Oncol. 2021; 11: 684961.
49. Xu X, Ye L, Araki K, Ahmed R. mTOR, linking metabolism and immunity. Semin Immunol. 2012; 24: 429-35.
50. Zhao L, Zhang H, Li N, Chen J, Xu H, Wang Y, et al. Network pharmacology, a promising approach to reveal the pharmacology mechanism of Chinese medicine formula. J Ethnopharmacol. 2023; 309: 116306.
51. Nogales C, Mamdouh ZM, List M, Kiel C, Casas AI, Schmidt HHHW. Network pharmacology: curing causal mechanisms instead of treating symptoms. Trends Pharmacol Sci. 2022; 43: 136-50.
52. Zhang HQ, Xie XF, Li GM, Chen JR, Li MT, Xu X, et al. Erianin inhibits human lung cancer cell growth via PI3K/Akt/mTOR pathway in vitro and in vivo. Phytother Res. 2021; 35: 4511-25.
53. Dobashi Y, Suzuki S, Matsubara H, Kimura M, Endo S, Ooi A. Critical and diverse involvement of Akt/mammalian target of rapamycin signaling in human lung carcinomas. Cancer. 2009; 115: 107-18.
54. Amornphimoltham P, Patel V, Sodhi A, Nikitakis NG, Sauk JJ, Sausville EA, et al. Mammalian target of rapamycin, a molecular target in squamous cell carcinomas of the head and neck. Cancer Res. 2005; 65: 9953-61.
55. Panwar V, Singh A, Bhatt M, Tonk RK, Azizov S, Raza AS, et al. Multifaceted role of mTOR (mammalian target of rapamycin) signaling pathway in human health and disease. Signal Transduct Target Ther. 2023; 8: 375.

56. Mossmann D, Park S, Hall MN. mTOR signalling and cellular metabolism are mutual determinants in cancer. Nat Rev Cancer. 2018; 18: 744-57.
57. Ma L, Li M, Zhang Y, Liu K. Recent advances of antitumor leading compound erianin: mechanisms of action and structural modification. Eur J Med Chem. 2023; 261: 115844.
58. Wei X, Liu J, Xu Z, Wang D, Zhu Q, Chen Q, et al. Research progress on the pharmacological mechanism, in vivo metabolism and structural modification of erianin. Biomed Pharmacother. 2024; 173: 116295.

Cite this article as: Yan L, Liu Y, Huang Y, Sun X, Jiang H, Gu J, et al. Erianin inhibits the proliferation of lung cancer cells by suppressing mTOR activation and disrupting pyrimidine metabolism. Cancer Biol Med. 2025; 22: 144-165. doi: 10.20892/j.issn.2095-3941.2024.0385